NCAR | EARTH OBSERVING LABORATORY

SWEX

NCAR/EOL ISFS Surface Meteorology and Flux Products Data Report

Prepared by Jacquelyn Witte - Data Manager

Dr. Steve Oncley - ISFS Lead Scientist

Earth Observing Laboratory
In situ Sensing Facility

NATIONAL CENTER FOR ATMOSPHERIC RESEARCH
BOULDER, COLORADO 80307-3000

Table of Contents

SWEX Principal Investigators

Leila Carvalho, University of California, Santa Barbara
Charles Jones, University of California, Santa Barbara
Gert-Jan Duine, University of California, Santa Barbara
Craig Clements, San Jose State University
Stephan De Wekker, University of Virginia
Joe Fernando, University of North Dakota
David Fitzjarrald, SUNY - Albany
Robert Fovell, SUNY - Albany
Zhien Wang, University of Colorado, Boulder
Loren White, Jackson State University

EOL ISFS Staff

ISFS Lead Scientist: Steven Oncley <oncley@ucar.edu>
Engineers: Chris Roden, Gary Granger, Isabel Suhr
Technicians: Anthony Weise
Data Managers/Associate Scientists: Jacquelyn Witte <jwitte@ucar.edu>, Matthew Paulus

Web References

SWEX Homepage: https://www.eol.ucar.edu/field_projects/swex
SWEX Field Catalog: https://catalog.eol.ucar.edu/swex
ISFS Homepage: https://www.eol.ucar.edu/node/152
Calculation of long-wave radiation:
https://www.eol.ucar.edu/content/calculation-long-wave-radiation

Visualization Resources

- NCharts: http://datavis.eol.ucar.edu/ncharts/projects/SWEX
- SWEX ISFS Daily Data Statistics and Plots

Related Documentation

ISFS netCDF File Conventions: ISFS netCDF File Conventions
ISFS Guides: https://www.eol.ucar.edu/content/isfs-guides

Citations

If these data are used for research resulting in publications or presentations, please acknowledge EOL and NSF by including the following citations, as appropriate:

Data Set

NCAR/EOL ISFS Team. 2023. SWEX: ISFS Surface Meteorology and Flux Products - georeferenced. Version 1.0. UCAR/NCAR - Earth Observing Laboratory. https://doi.org/10.26023/XDKV-QXC2-1Y0J. Accessed 04 Feb 2023.

The ISFS Platform

NCAR - Earth Observing Laboratory. (1990). NCAR Integrated Surface Flux System (ISFS). UCAR/NCAR - Earth Observing Laboratory. https://doi.org/10.5065/D6ZC80XJ.

Acknowledgement

Users of EOL data are expected to add the following acknowledgement to all of their publications, reports and conference papers that use those data:

“We would like to acknowledge operational, technical and scientific support provided by NCAR’s Earth Observing Laboratory, sponsored by the National Science Foundation.”

Overview

The Sundowner Wind Experiment (SWEX) was conducted in the Santa Ynez Mountains in Santa Barbara County, California for the period 01 April - 15 May 2022. ISFS operated 18 10-meter towers with a full suite of flux and meteorological monitoring sensors and soil sensors.

Data Set Description

Project Period: 01 April - 15 May 2022
Data set Period: 01 April - 15 May 2022

Center Location: Santa Barbara, CA
Data layout: ISFS netCDF File Conventions
Data file frequency: Daily
Data version: v1.0
Data access: public

5-minute data set

Data format: netCDF3
File name format: isfs_swex_5min_qc_geo_tiltcor_YYYYmmDD.nc
Time resolution: 5-minute

High Rate data set

Data format: netCDF3
File name format: isfs_swex_hr_qc_geo_tiltcor_YYYYmmDD.nc
Time resolution: - Varies from 50 ms for 20 Hz sensors to 1s for 1 Hz sensors.
- Refer to Table 2 for sampling rates.

Data set name	SWEX: ISFS Surface Meteorology and Flux Products - georeferenced
DOI	https://doi.org/10.26023/XDKV-QXC2-1Y0J

Site Description

18 flux towers operated in and around Santa Barbara and the Santa Ynez Mountains as far north as the Los Padres National Forest and west as Gaviota State Park. Refer to **Table 1** for site locations and sensor configurations. **Figure 1** shows relief map rendition of the sites deployed around the Santa Barbara region.

Figure 1. Google Map rendering of site locations is provided below.

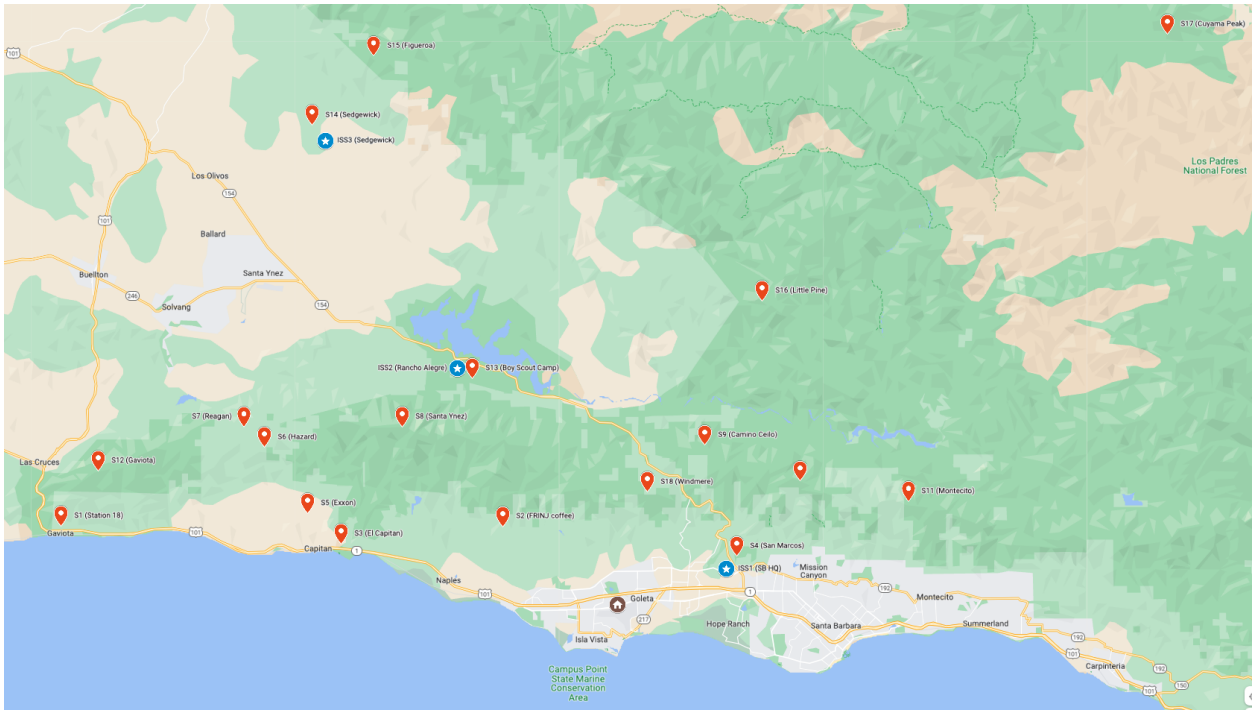

Table 1. Sites and locations. The abbreviated short name is the netCDF sitename definition.

Site	Short Name	Latitude	Longitude
Station 18	s1	34.4758272	-120.2146195
FRINJ coffee	s2	34.475533	-119.920261
El Capitan	s3	34.465974	-120.027886
San Marcos	s4	34.459259	-119.764333
Exxon	s5	34.482840	-120.05044
Hazard	s6	34.519034	-120.078933
Reagan Ranch	s7	34.5302339	-120.0927446
Santa Ynez	s8	34.530111	-119.987306
Camino Cielo	s9	34.520205	-119.785680
La Cumbre	s10	34.500530	-119.722015
Montecito	s11	34.4893769	-119.6499334
Gaviota	s12	34.5059778	-120.1899385
Boy Scout Camp	s13	34.556841	-119.940481
Sedgwick	s14	34.6955305	-120.0471357
Figueroa	s15	34.7334442	-120.006304
Little Pine	s16	34.599367	-119.747283
Cuyama Peak	s17	34.745244	-119.477392
Windermere	s18	34.494511	-119.824009

Flux Tower Instrumentation

All ISFS SWEX towers were similarly instrumented to measure basic meteorology, eddy covariance fluxes, radiation, and soil heating and moisture. All flux towers reached a nominal height of 10m. Refer to **Photo 1** for a visual reference. The radiometers and soils were set-up separately on tripods (refer to **Photo 2** for a visual reference). The standard 5-min and high rate ISFS products include measurements from the sensors listed in **Table 2**.

All wetness sensors were coupled to each radiometer to filter incidences of moisture on the sensor dome, i.e. dew, rain, or snow.

Table 2. ISFS sensors and description. A subset of these sensor products (those sensors in **bold**) are in the high rate datasets.

Instrument	Manufacturer	Nominal height	Samples/ s
Integrated Net Radiometer	4-component Hukseflux NR01	1 m	0.2
Wetness	Decagon	1 m	0.2
Soil temperature profile sensor	NCAR 4-level Tsoil	0.6 cm, 1.9 cm, 3.1 cm, 4.4 cm	0.2
Soil thermal properties	Hukseflux TP01	2.5 cm	0.2
Soil Moisture	Meter EC-5	2.5 cm	0.2
Heat flux plate	REBS HFT	5 cm	0.2
Disdrometer	OTT Parsivel2		0.02
2D sonic anemometer	**Gill WindObserver**	**10 m**	**10**
3D sonic anemometer	**Campbell Scientific CSAT3****	**5 m**	**20**
H2O/CO2 Open-path InfraRed Gas Analyzer (IRGA)	**Campbell Scientific (combination of EC100 and EC150)**	**5 m**	**20**
Hygrothermometer	**Sensirion SHT85**	**2 m**	**1**
Nanobarometer	**Paroscientific 6000**	**5 m**	**20**

**With the optional CSAT3A sonic anemometer head to couple with the IRGA EC150.

Photo 1. Photos showing a typical instrument towered set-up. Top left: s4 (San Marcos Foothills Preserve). Top right: s15 (Figueroa Mountain). Bottom Left: s14 (Sedgwick Reserve). Bottom right: s9 (E Camino Cielo)

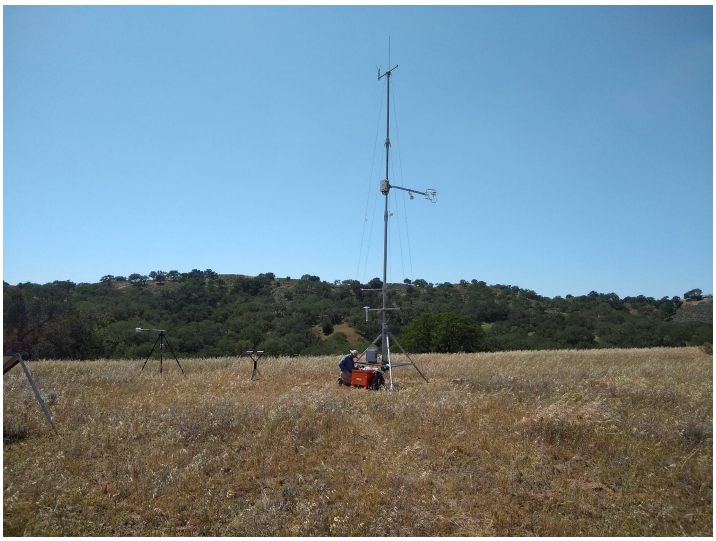

Photo 2. Radiometer set-up on tripod with soils buried at its base shown for s15 (Figueroa Mountain) - Top and s10 (La Cumbre).

3D Sonic Anemometer Geographic Coordinates and Tilt Corrections

In order to report winds in geographic coordinates, the orientation of the instrument relative to true north needs to be known. With an azimuth angle measured along the boom, the orientation is known since every anemometer head is rigidly attached to the boom in a captive manner. For SWEX, a hand-held compass was used to measure the direction along the 3D sonic anemometer boom (nominally 5 m height) looking into the tower with respect to the magnetic north. From these measurements, the 10 m 2D sonic anemometer orientations were then calculated, as those booms are affixed at a 90 degree angle from the 3D sonics. Refer to **Table 2** for compass measured boom angles. Compass angles have been converted to true headings using a magnetic declination of 12.3 degrees east.

Typically, we estimate the sonic tilt angles with respect to the flow through the sensors from the archived wind data using the planar fit technique described in Wilczak, Oncley, and Stage, 2001, "Sonic Anemometer Tilt Correction Algorithms," Boundary Layer Meteor., 99, pp. 127-150. These data sets are labeled as ‘planar’.

The SWEX towers were set-up to face prevailing winds on hilltop slopes with uneven terrain making accurate readings of the tilt of the 3D sonic anemometer not possible. Furthermore, by adding a tilt correction we would be erasing/canceling orographic effects, as prevailing winds will often be coming into the sonic at an angle following the slope of the terrain.

We provide the planar fits in **Table 3**, **however we have not applied these fits**. The local slope direction varied over the domain, resulting in planar fits over a large range of degrees. Refer to the companion photographic documentation for visualizations of the tower set-up scheme for each site.

A list of reference material below provides information on tilt corrections and wind coordinates using compass bearings.

- Sonic tilt corrections - Processing of sonic anemometer data.
- Wind direction quick reference - Explanation of the wind coordinate system.
- Wilczak, J.M., Oncley, S.P. & Stage, S.A. Sonic Anemometer Tilt Correction Algorithms. Boundary-Layer Meteorology 99, 127–150 (2001). https://doi.org/10.1023/A:1018966204465

Table 3. Anemometer orientations by site determined by compass bearings. Compass measurements of the boom angle measured between the vertical tower pole and centerline of the boom on which the anemometer is mounted. 3D sonics were mounted at a nominal height of 5m.

Site short name	Compass Bearing into the boom [deg]	Lean [deg]	Lean Azimuth [deg]	w offset [cm/s]
s1	123	6.6	-5.4	-1
s2	133	6.8	-68.0	10
s3	136	5.7	-28.1	0
s4	113	4.1	-0.2	-1
s5	136	7.0	-178.8	23
s6	135	17.5	17.1	15
s7	131	5.1	-24.2	3
s8	137	14.5	119.3	-7
s9	136	11.5	67.5	36
s10	137	3.4	-136.7	1
s11	136	7.2	107.3	-1
s12	141	2.6	-168.0	6
s13	118	3.9	151.2	-1
s14	111	1.8	-4.7	2
s15	142	8.8	-67.1	6
s16	121	6.2	-53.0	0
s17	121	17.2	101.5	35
s18	135	10.5	5.1	1

Data File Contents

Data files are provided in netCDF3 format. Research parameters contained in the 5-minute and high rate data are provided below.

ISFS netCDF File Conventions

Refer to the ISFS netCDF File Conventions for a readme guide to understanding how ISFS netCDF data files are constructed and how the variables are defined.

Also, please note that 5-minute averaging often is insufficient to capture all of the scales of turbulence contributing to the total flux, especially in unstable (daytime) conditions. We recommend averaging longer, which can easily be done from the 5-minute average data, using the procedure described in combining short-term moments.

SWEX Variable name convention

Variable naming convention follows the convention of <variable>_<height>_<site shortname> or <variable>_<site shortname>. For example, Spd_10m_s10 refers to the 2D anemometer wind speed at site s10, while spd_s10 refers to the 3D anemometer wind speed at site s10. A list of all the research variables are below.

Meteorological Variables

Variable name	Quantity Measured	unit	Instrument
P	Barometric Pressure	mb	Paroscientific 6000
T	Air Temperature	degC	Sensirion SHT85
RH	Relative humidity	%	Sensirion SHT85
U	Wind U component	m/s	2D Gill WindObserver
V	Wind U component	m/s	2D Gill WindObserver
Spd	Wind speed	m/s	2D Gill WindObserver
Dir	Wind direction	deg	2D Gill WindObserver
Tc	2D sonic temperature	degC	2D Gill WindObserver

3D Sonic Anemometer Variables

Instrument - Campbell Scientific CSAT3

Variable name	Quantity Measured	unit
u	Wind U component	m/s
v	Wind V component	m/s
w	Wind W component	m/s
spd	Wind speed	m/s
dir	Wind Direction	deg
tc	Virtual air temperature from speed of sound	degC
ldiag	logical diagnostic applied, 0=OK, 1=one or more non-zero diag bits	none

CO_2 and H_2O Open-Path Gas Analyzer Variables

Instrument - Campbell Scientific combination of EC100 and EC150 models

Variable name	Quantity Measured	unit
h2o	Water vapor density	g/m^3
co2	CO2 density	g/m^3
Pirga	Barometric pressure	mb
Tirga	Air temperature	degC
irgadiag	Sensor diagnostics applied, 0=OK, 1=one or more non-zero diag bits	none

Radiation Variables

All the satellite sites used the Hukesflux NR01 radiometers mounted on tripods at 2m. Calculation of long-wave radiation from the thermopile and case temperatures can be found here: https://www.eol.ucar.edu/content/calculation-long-wave-radiation

Radiation data are not included in the high rate data due to the coarse time resolution. Refer to **Table 2** for sampling rates.

Variable name	Quantity Measured	unit	Instrument
Rsw_in	Incoming Shortwave	W/m^2	Hukesflux NR01
Rsw_out	Outgoing Shortwave	W/m^2	Hukesflux NR01
Rpile_in	Incoming Thermopile	W/m^2	Hukesflux NR01
Rpile_out	Outgoing Thermopile	W/m^2	Hukesflux NR01
Tcase	Case temperature	degC	Hukesflux NR01
Rlw_in	Incoming Longwave	W/m^2	Hukesflux NR01 (derived)
Rlw_out	Outgoing Longwave	W/m^2	Hukesflux NR01 (derived)
Rsum	Signed sum of Rsw and Rlw (otherwise known as Rnet)	W/m^2	Hukesflux NR01 (derived)
Tsfc_pyrg	Surface temperature from Rlw_out, using emissivity=0.98	degC	Hukesflux NR01 (derived)
Wetness	Leaf Wetness	V	Decagon

Soil Variables

Soil data are not included in the high rate data due to the coarse time resolution. Refer to **Table 2** for sampling rates.

Variable name	Quantity Measured	unit	Instrument
Gsoil	Soil heat flux	W/m^2	REBS HFT
Qsoil	Soil moisture	m^3/m^3	Meter EC-5
Tsoil	Soil temperature	degC	NCAR 4-level Tsoil
Lamda (formerly Lambdasoil)	Soil thermal conductivity	W/m/DegK	Hukseflux TP01
Tau63	Decay time constant	s	Hukseflux TP01
asoil	Soil thermal diffusivity	m^2/s	Hukseflux TP01 (derived)
Cvsoil	Soil heat capacity	$J/(m^3\ K)$	Hukseflux TP01 (derived)
Gsfc	Surface value of soil heat flux	W/m^2	HFT; Tsoil; TP01 (derived)

Soil variables with cr extension

Sites s1 and s4 contained an extra set of soil sensors defined in the netcdf files with the "_cr_" extension in the variable name, i.e. Qsoil_cr_s1. These are test sensors that use a new analog to digital converter (ADC) chip that has a lower temperature sensitivity and does not require a temperature calibration, compared to the standard soil sensor system used at all the SWEX sites. Based on laboratory tests, the new "_cr" ADC performed the same or better than the standard converters. The observable differences presumably are due to soil variability and low soil moisture leading to poor sensor and soil contact.

Precipitation Variables

Precipitation data are not included in the high rate data due to the coarse time resolution. Refer to **Table 2** for sampling rates.

Instrument - OTT Parsivel2 Disdrometer

Variable name	Quantity Measured	unit
Rainr	Rain rate	mm/h
WX	Weather code according to SYNOP code*	-
Vis	MOR visibility in precipitation	m
N	Particle count	-

*For interpretation, refer to Appendix D of the Parsivel2 Operation Manual

Dimension Variables

Variable name	Quantity Measured	unit
base_time	seconds since 1970-01-01 00:00:00 00:00	s
time	seconds since 2022-04-01 00:00:00 00:00	s

Higher Moments

We provide a long list of 2nd and 3rd moments among the winds, h2o, and co2. They follow the naming convention:

2nd moment: varname_varname__

3rd moment: varname_varname_varname__

For example,

```
float u_tc__sp(time) ;
        u_tc__sp:_FillValue = 1.e+37f ;
        u_tc__sp:long_name = "2nd moment" ;
        u_tc__sp:short_name = "u\'tc\'.sp" ;
        u_tc__sp:units = "m/s degC" ;
        u_tc__sp:counts = "counts_sp" ;

float w_w_tc__sp(time) ;
        w_w_tc__sp:_FillValue = 1.e+37f ;
        w_w_tc__sp:long_name = "3rd moment" ;
        w_w_tc__sp:short_name = "w\'w\'tc\'.sp" ;
        w_w_tc__sp:units = "(m/s)^2 degC" ;
        w_w_tc__sp:counts = "counts_sp" ;
```

Refer to the ISFS netCDF document which provides further detail on the ISFS instruments and their parameters, the netCDF naming convention, time sampling, and attributes.

Flux corrections

The calculation of certain fluxes is a bit more involved that just the covariance, due to the spatial separation of some sensors, the sensitivity of the sonic anemometer temperature to humidity, and density effects. These corrections are applied to create the following variables:

Variable name	Quantity Measured	unit
w't'	Covariance of vertical velocity with temperature (not acoustic temperature)	degC m/s
w'h2o'	Covariance of vertical velocity with humidity	m/s g/m^3
w'co2'	Covariance of vertical velocity with carbon dioxide	m/s g/m^3
H	Sensible heat flux	W/m^2

LE	Latent heat flux	W/m^2

Data Collection and Processing

All sensors were sampled independently with a Linux-based Data System Module or DSM. Data were stored directly onto USB sticks provided for every DSM. At SWEX, all DMSs used cell modems to transmit raw data in real time to the ISFS base trailer. Data were also transmitted from the base trailer to servers at EOL for local storage and added back-up. Data processing was performed by the in-house created-data acquisition software called NIDAS.

NIDAS (NCAR In-situ Data Acquisition Software) handles the data processing for all ISFS measurement systems. This is linux-based software produced by Gordon Maclean, formerly at NCAR/EOL. Each sensor is sampled independently. A time tag is assigned to each sample at the moment it is received, based on a system clock synchronized to GPS time. Minimal data interpretation is performed to differentiate individual messages from a sensor, assembling the data exactly as it was received into a sample, with the associated time-tag and an identifier of the sensor and data system. The concatenated stream of samples from all sensors is then passed on for archival and further processing.

NIDAS reads a series of configuration and calibration files that contain pertinent sensor metadata and, more importantly, any input variables that are to be applied to the data either during operations or in post-processing. NIDAS will also apply quality control flags and filters, and thresholds. To generate the 5-minute average and high rate data sets, NIDAS reads the variables from the raw information, applies calibrations and quality control filters, generates 5-minutes averages for those data sets, then writes the variables to a netcdf.

- Further introduction to NIDAS and access to the software can be found on its GitHub Wiki.
- NIDAS version used in these data sets is v1.2-1667.

Data Availability

Figure 2 shows the percent of 5-minute ISFS sensor data remaining per variable after all quality checks and filters have been applied. The Hukseflux TP01, measuring thermal conductivity (Lambdasoil) and decay time (tau63), at site s9 behaved as though it was exposed to the air since it was installed (data availability is 22.6%). These time series were removed 5 May 2023 when the sensor was replaced. The gas analyser at site s16 was bad and data were removed until the IRGA was replaced on 5 May 2023 (data availability is 22.6%). The lower rates of data availability in the NR01 radiometer data (Rsw, Rlw) are due to filtering of the wetness on the sensor's lens.

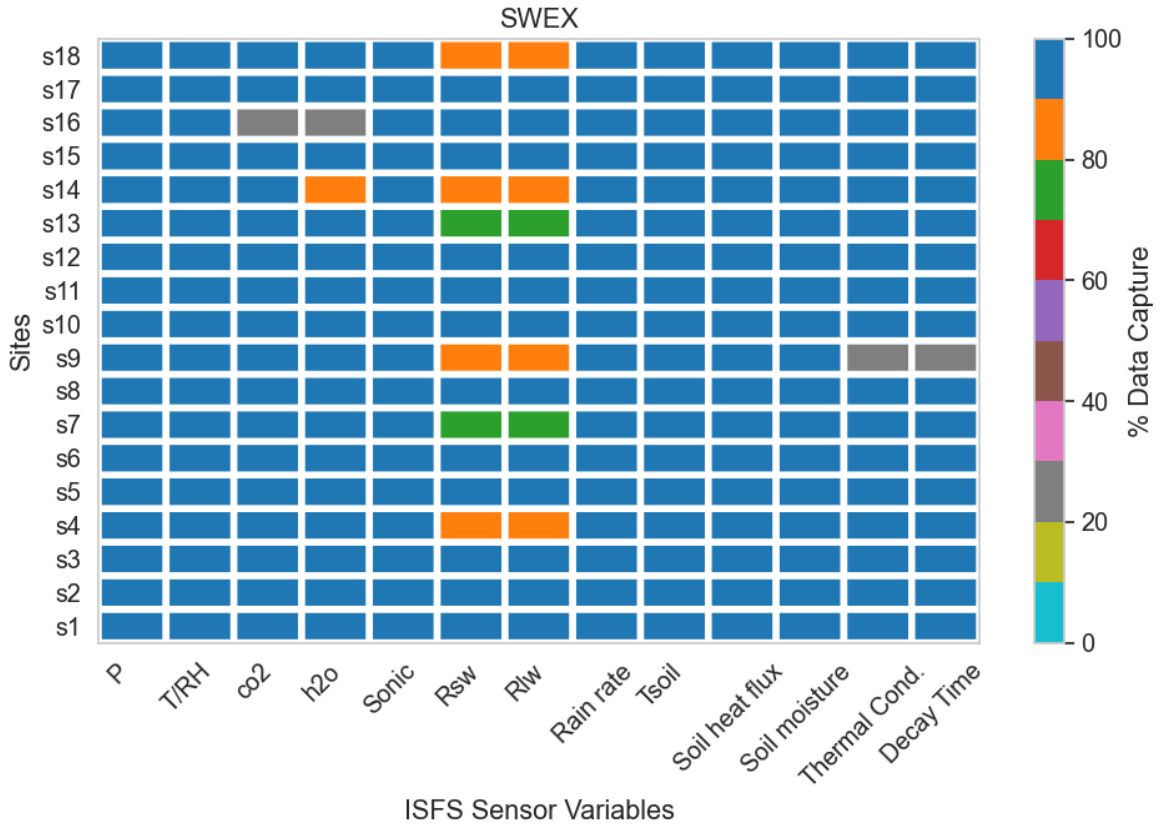

Figure 2. Percent of data available during SWEX. Most major ISFS sensor data sets are included.

Data Gaps

Small data gaps occur from time to time in a given sensors' data stream. These may be due to

- Loss of GPS signal when rebooting due to loss of power due to maintenance, i.e. servicing sensors.
- Sensor thresholds on the data.
- Status or error messages from the sensor

Data Quality

ISFS performed data quality checks on all sensors. Below we provide summaries of the QC workflow for each sensor.

Tower lowering/raising

We did our best to keep a record of the dates and times when towers were lowered for maintenance.

Table 4. Dates and time when towers were lowered for maintenance. Start and end times are taken from the 5-minute data set in UTC.

Site	Start time	End Time	Reason
s5	15 Apr 02:42	15 Apr 23:37	Fallen tower due to high winds. Strong winds developed across the western, coastal sites in the late afternoon. Winds reached ~20 m/s at s5 before it dropped off the network. Replaced 2D and 3D sonics plus the EC100, and the gas analysers.
s14	08 Apr 20:37	08 Apr 21:02	Replaced EC150 desiccant bottle
s14	03 May 23:22	03 May 23:47	Corrected orientation of 3D sonic
s16	24 Apr 18:57	24 Apr 19:52	Replaced EC150 desiccant bottle
s16	05 May 19:32	05 May 20:17	Replaced EC150

Photo 3. Site 5 showing the fallen tower (left) after high winds blew it down. The stakes on the “northwest” leg were pulled from the fairly loose, sandy soil. Upon visual inspection the only damage was to the EC100 (right), which was dented after landing on a rock. The re-elevated mast was resecured with a 70 pound bag of sand on each tripod leg.

Barometers

The Paroscientific nanobarometers were connected to NCAR-built quad-disk probes, based on the design by Nishiyama and Bedard (1998), and all pressure sensors worked as expected. No problems noted during operations. No problems were found during QC processing. No sensors were replaced during operations. Time series of all nanobarometers operating are plotted in **Figure 3**. Differences in the average pressures are due to the station elevation.

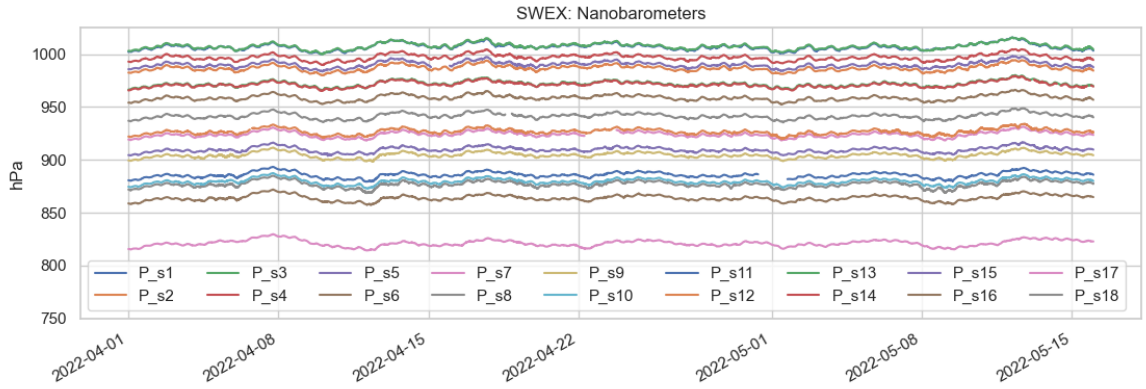

Figure 3. Time series of nanobarometers by site.

Hygrothermometer (T, RH)

Each tower used ventilated temperature/relative humidity sensors. The fan speeds in the sensor housings were collected and used as an indicator that the ventilation fans were functioning as expected. In general, the measurements were fairly stable. All the TRH sensors performed well. TRH casing was replaced at s1 on 05 May due to a broken fan. No further problems noted during operations. No problems were found during QC processing. Time series of all TRH sensors by site are plotted in **Figure 4**.

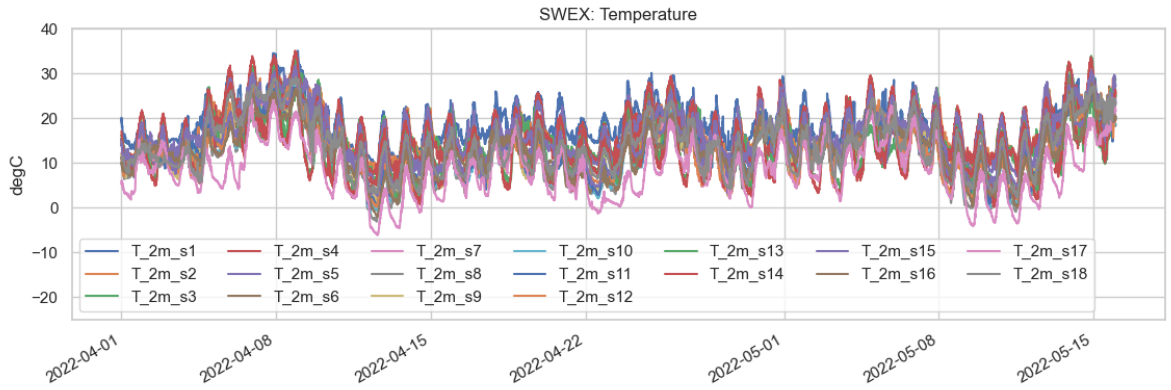

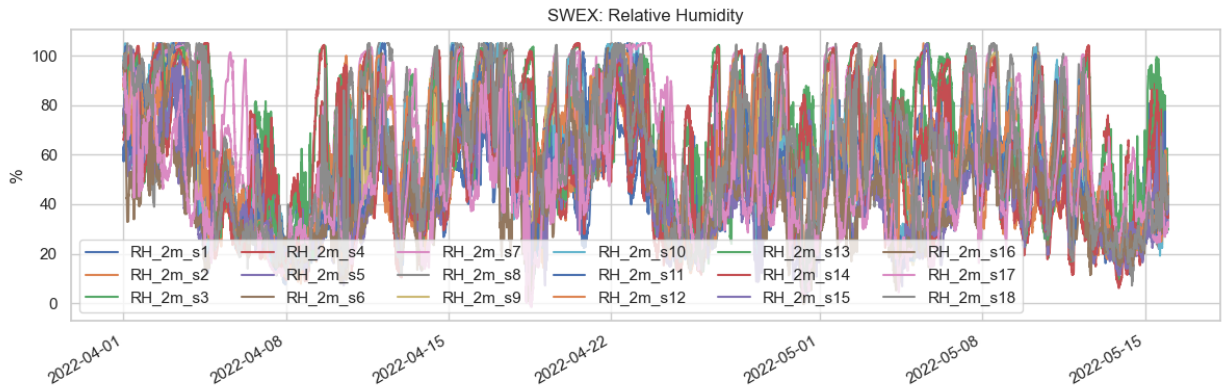

Figure 4. Time series of TRH sensors by site.

TRH Calibrations

Calibrations were done on the TRH sensors in the EOL Calibration Laboratory https://www.eol.ucar.edu/node/2652. Temperature oil baths were used to calibrate the temperature sensors and a Humidity Chamber to calibrate the relative humidity sensors. Three constant temperatures were used to calibrate the RH; 1°C, 20°C, and 40°C. To evaluate the hysteresis effect, the RH chamber was allowed to slowly increase from zero to near-100% then decrease back down to the zero. This process takes three days to complete. Eight RH probes were calibrated at a time. An example of a calibration plot is shown in **Figure 5**.

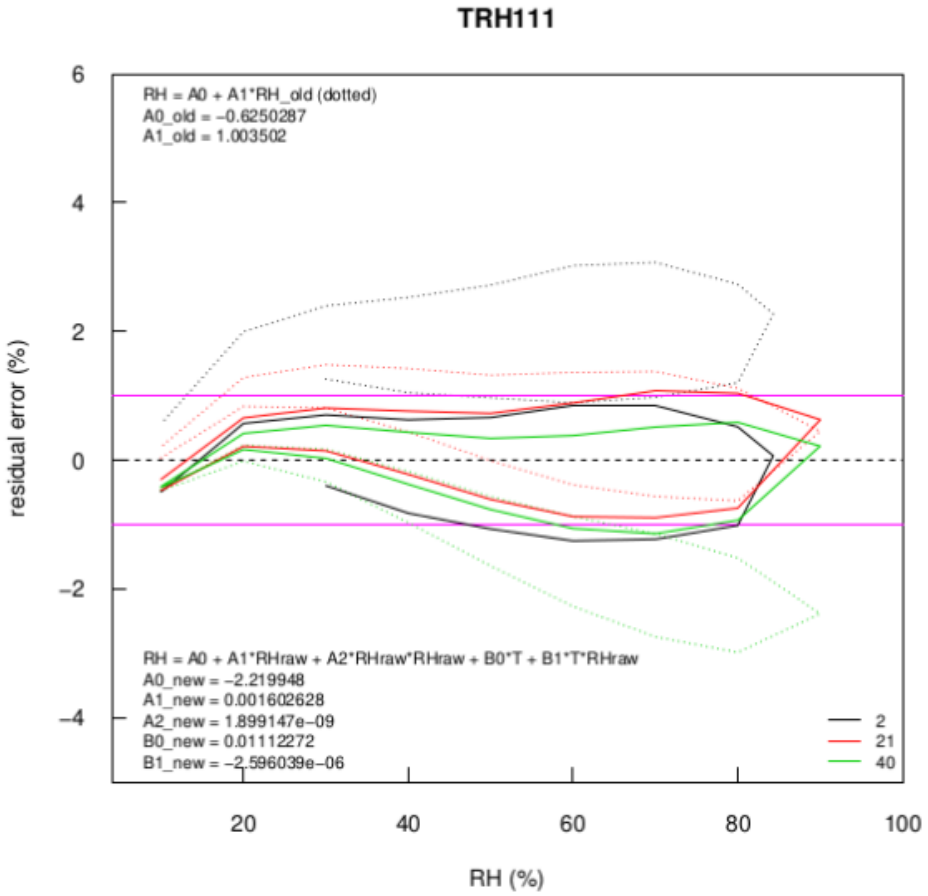

Figure 5. Post-calibration of RH for TRH sensor 111 at constant temperatures (1°C-black, 20°C-red, and 40°C-green). The curved shape is the result of measuring the increase then decrease of the known RH source at each temperature. The difference between the upper and lower bounds of the curve defines the hysteresis effect. Dotted lines are the percent residual error relative to a known source of RH before calibration. The solid lines are the adjustments to the fit to reduce the error to within 2%. Post campaign calibrations are the average of the three unadjusted curves and are included in the plot as A0_old (offset) and A1_old (gain). The final calibrated fits are the solid lines and fits to the average of post-calibrations are provided on the bottom left with additional terms to the fit equations that accounts for the temperature dependence.

Pre-calibrations were completed in October and November 2021. All humidity sensors were calibrated to within ± 2% accuracy and all temperature probes were calibrated to within the expected error of ± 0.1°C. Post-calibrations were completed by August 2022.

The calibration fits applied to the RH and T references are provided in **Table 5**. For the temperature probes, we applied calibration corrections to s1, s8, and s11 which measured outside the expected error of +/- 0.1°C. We applied an RH correction at s1 which recorded an

overall error of 22%. An overall hysteresis effect of 1% at constant T=1°C was observed during RH calibrations.

Table 5. Post-calibration linear slope and offset fits to RH and T based on equation *probe* = *A0* + *A1*probe_raw*. These calibration corrections were applied to the quality controlled data.

Site	Serial No.	RH fits	T fits
s1	45	A0 = -0.4237104 A1 = 1.229809	A0 = -1.7752 A1 = 1.0108
s8	11		A0 = -0.4611 A1 = 1.0042
s11	42		A0 = -0.32335 A1 = 1.002

Radiometers

All sites used the NR01 radiometers mounted on tripods at nominal heights of 2m. A wetness sensor was attached close to the sensors to record moisture levels.

Data have been filtered for

- Spikes
- Moisture on the lens due to dew or precipitation as measured by the wetness sensors mounted on the NR01 radiometers.

We used the wetness sensor, mounted close to each radiometer set, to filter for moisture on the radiometer lens. We used a threshold of wetness > 0.27 V to filter for sites s1, s3, s4, s6, s9, and s10. For all the other sites we used a threshold of wetness > 0.2 V. Different threshold values are used due to two generations of front-end electronics for this sensor that use different excitation voltages for these sensors.

Refer to **Figure 2** for final data availability after quality checks for the ISFS-controlled sensors. Calculations of long-wave radiation using the Rpile and Tcase variables as described here: https://www.eol.ucar.edu/content/calculation-long-wave-radiation have been been added to the 5-minute NetCDF files, along with the sum of all four radiation components (net radiation). The radiative surface temperature calculated from Rlw_out is also added to these files.

Data notes:

Site s18 (Windermere) - There is data gap April 14-16 when the mote stopped. A power cycle of the mote during a site visit on the 16th brought the radiation sensor back up.

Otherwise, no other problems were noted during operations. No sensors were replaced during operations.

2-D Sonic anemometer - Gill WindObserver

In the standard ISFS set-up using the PAM tripods, the 2D Gill's booms are perpendicular to the 3D CSAT booms. At SWEX the 2D sonics were set-up to be approximately 90 degrees counterclockwise from the 3D sonic orientation, except for site s4 (90 degrees clockwise). Refer to **Photo 4** for a visual guide. The wind directions of both sonics were compared to examine possible flow distortions in the 2D Gill due to slight offsets in its orientation relative to the CSATs, rather than due to terrain features. The CSATs are the reference because their orientation has been measured and adjusted to geographic coordinates using compass bearings. Only s12 (Gaviota site) was shown to have an offset requiring an additional adjustment of -11 degrees relative to the CSAT azimuth.

Data notes:

Site s5 (Exxon Mobil) - 2D sonic was replaced on 14 April, 2022 due to the tower collapsing under heavy winds.

Photo 4. Photos of s2 (left) and s5 (right).

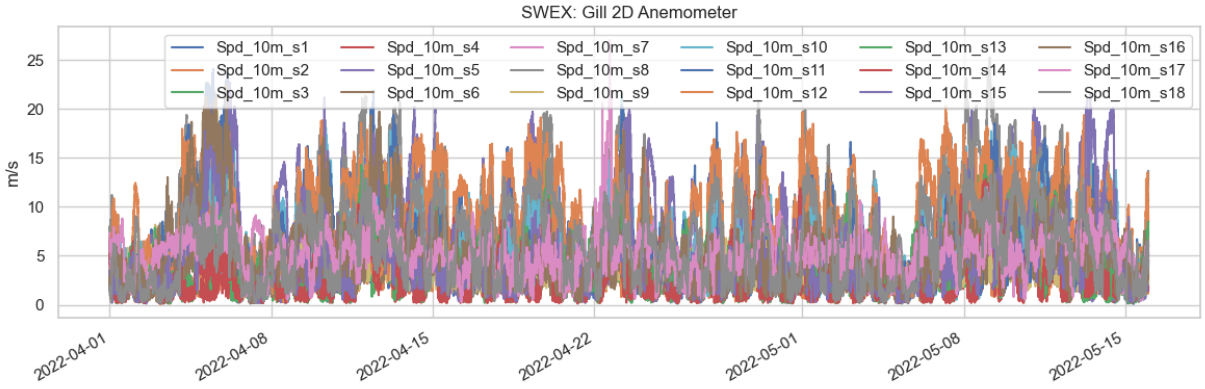

Figure 6. Time series of 2D anemometers by site.

3-D Sonic anemometer - CSAT3

CSAT3 sonic anemometers were used for turbulence measurements on all towers. The orientation of each sonic was calculated using a handheld compass. Windrose plots comparing the 2D and 3D anemometers can be found in **Appendix A**.

In addition, winds blowing through the mast and along the boom may typically be removed from the dataset, however in this case they were left in. This decision was made due to the prevalence of winds from these directions and a desire to not throw out data. Therefore winds coming from directions within 15 degrees of the compass bearing into the boom minus the magnetic declination of 12.3 degrees (**Table 3**) should be used with caution.

Data notes:

Site s5 (Exxon Mobil) - 3D sonic was replaced on 14 April, 2022 due to the tower tipping under heavy winds.

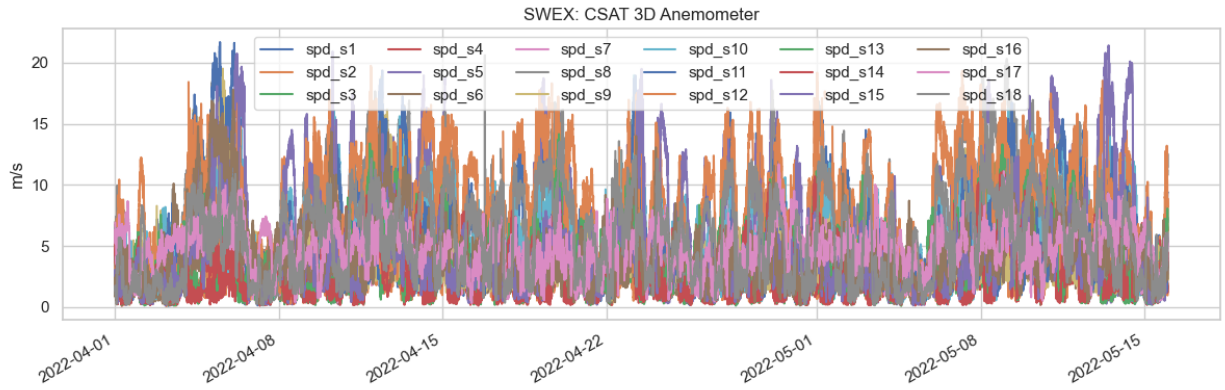

Figure 7. Time series of 3D anemometers by site.

Sonic Calibrations

Sonic anemometers performed calibration checks in an environmental chamber that operated over a defined stated temperature range (-30°C to +50°C). The anemometers were calibrated with three orientations (on the x, y, z axes) and the u component was examined. Overall, the u component measured deviations between 0.0 cm/s and 0.3 cm/s with a standard deviation of +/- 0.1 cm/s. Calibrations were conducted in July and August 2022. All sonics performed within specification and no adjustments were made.

H_2O/CO_2 Infrared Gas Analyser (EC150 IRGA)

CSAT3 was coupled with an infrared absorption gas analyzer (EC-150 IRGA) to measure H_2O and CO_2.

The sensors were filtered for

- irgadiag not equal to 0
- Negative spikes in H_2O that are not captured by the internal diagnostics.

Data notes:

EC150 variables should be set to the not-a-number fill value for when irgadiag is non-zero. We have noticed this does not happen in all cases. We recommend the user re-apply the irgadiag ≠ 0 filtering criteria when using these data.

Site s5 (Exxon Mobil) - EC150 was replaced on 14 April 2022 due to the tower tipping under heavy winds. This was done as a precaution, even though the sensor was still functioning.

Site s7 (Reagan Ranch) - co2 was biased high relative to all other sites' time series. We subtracted an offset of 8 g/m^3.

Site s14 (Sedgwick Reserve) - Replaced desiccant bottle 08 April 2022. Data before that date and for a day after may be suspect.

Site s16 (Little Pine) - EC150 data was removed until 05 May 2022 when the sensor was replaced.

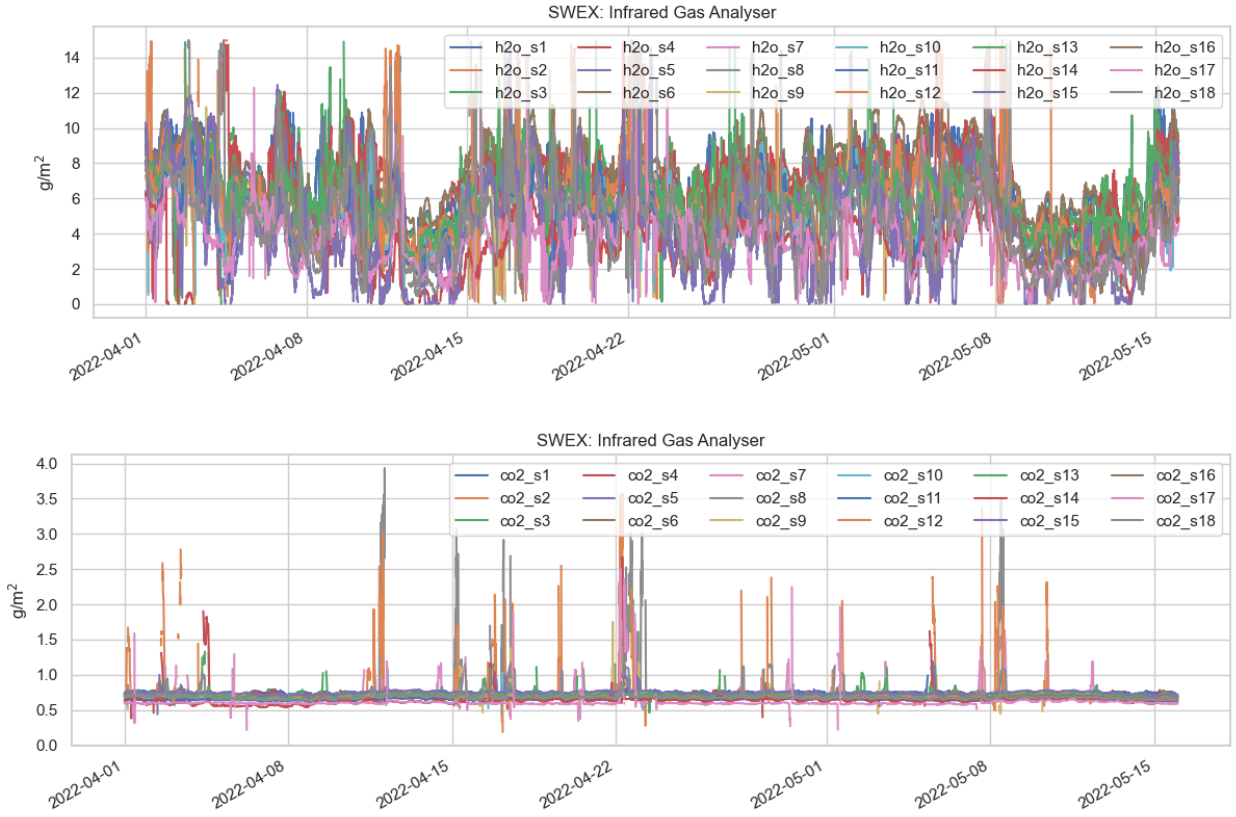

Figure 8. Time series of h2o (top) and co2 (bottom) by site.

Calculations of derived sensible and latent heat fluxes, as described in: [corrections to sensible and latent heat flux] have been added to the 5-minute NetCDF files.

Soils

All soil sensors (NCAR 4-level Tsoil, Meter EC-5 Qsoil, REBS HFT Gsoil, and Hukseflux TP01 thermal properties) were buried at 0 – 5 cm layer near the base of towered sites. Refer to documentation on the installation of soil sensors for more details.

Heat flux, Gsoil

Site s15 - We replaced the Gsoil probe that stopped reporting 6 April 2022.
No other problems noted during operations. No problems were found during QC processing.

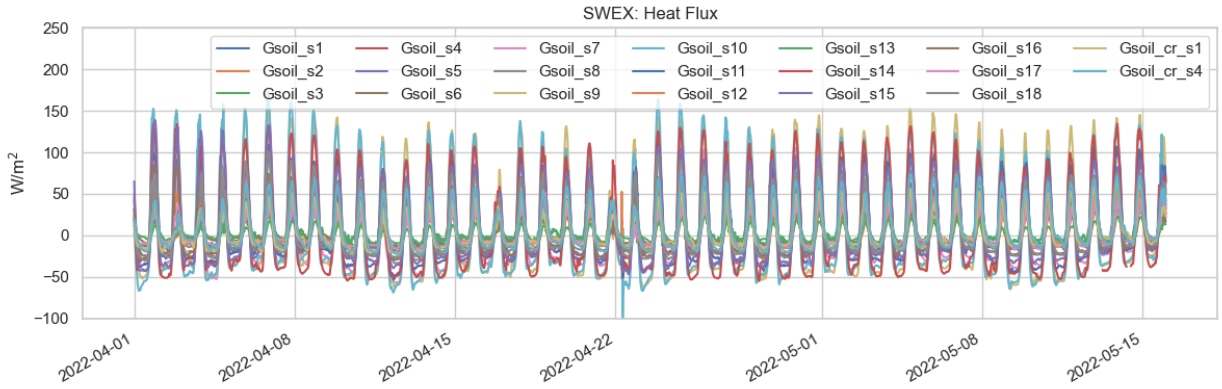

Figure 9. Time series of Gsoil at each site.

Calculations of the heat flux at the surface, corrected for the Phillip correction and heat storage within the 0--5 cm layer of soil using the Tsoil and TP01 data and as described in calculation of soil heat flux at the surface have been added to the 5-minute NetCDF files.

Soil Temperature, Tsoil

Tsoil sensors were installed at depths of 0.6 cm, 1.9 cm, 3.1 cm and 4.4 cm. No problems noted during operations. No sensors were replaced during operations.

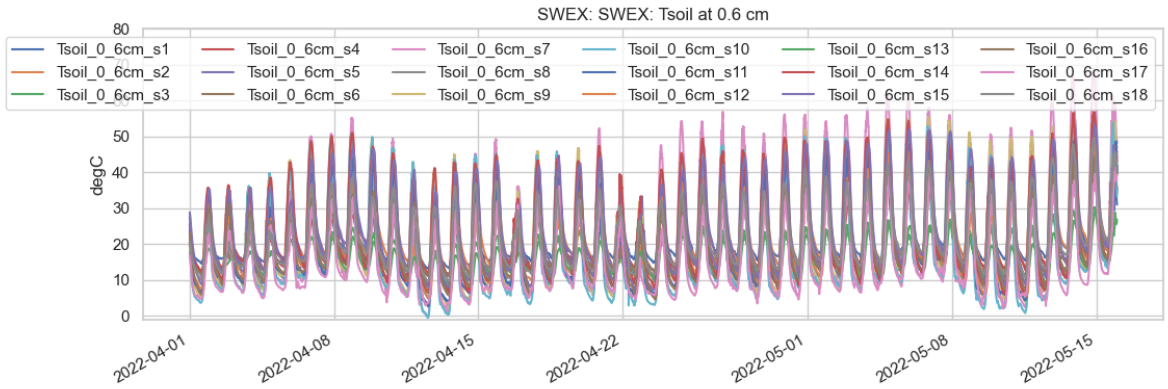

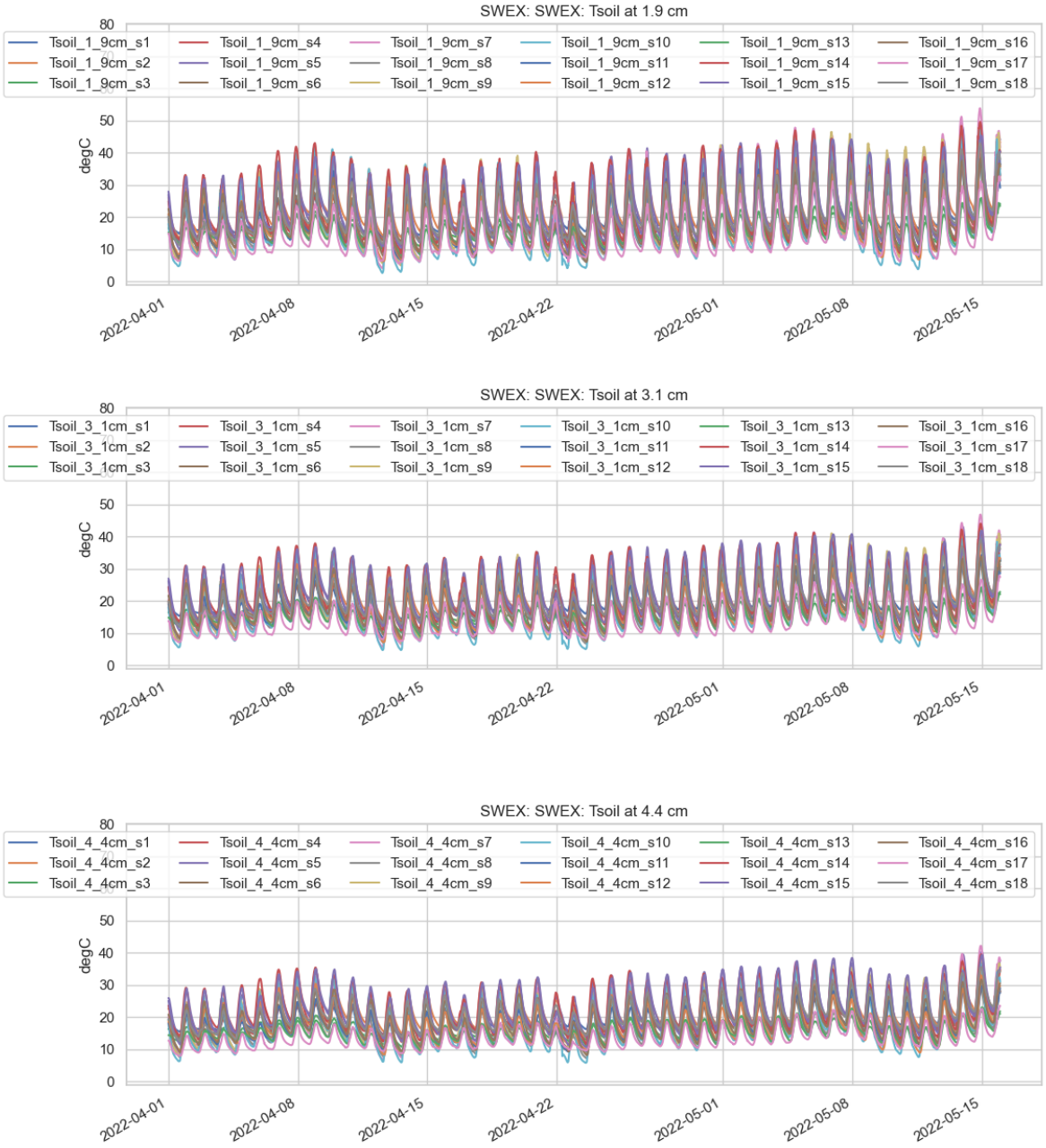

Figure 10. Time series of Tsoil at each height level.

Soil Moisture, Qsoil

The soil moisture sensor (Qsoil) was installed at a depth of 2.5 cm. We used the manufacturer's calibration values for potting soil.

Three soil samples were taken at each site during the course of the field project. These samples were used to measure soil moisture content by the gravimetric method: a fresh soil core sample is weighed, oven dried until there is no further mass loss, and then reweighed. The moisture content is expressed as mass of water per mass of dry soil. **Figure 11** are the comparisons between Qsoil and the gravimetric results. We applied corrections based on the fits to the gravimetric soil moisture for all sites, except s6, s8, s9, s10, s14, s15, s16, and s18 which were inconclusive. **Figure 12** shows the final Qsoil time series for all sites after corrections have been applied. The overall effect of applying the adjustments was to elevate Qsoil values. Staff reported that soil conditions were dry, soft, and gravelly throughout the project. At times, several attempts were required to get a decent sample. This can account for the disagreement at several sites seen in **Figure 11**.

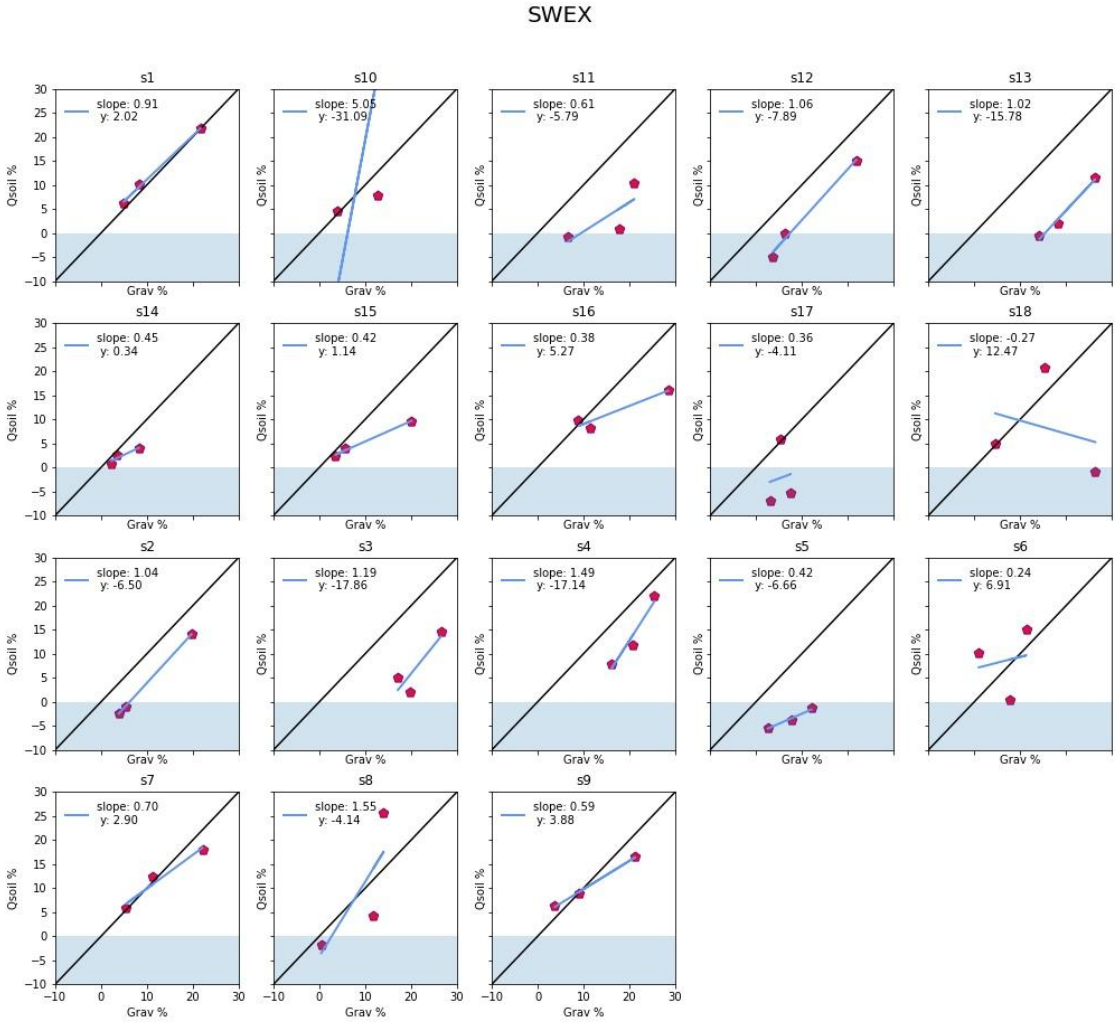

Figure 11. Comparison of Qsoil to the gravimetric soil moisture for each site. The linear fits at most sites were used to correct the low bias in Qsoil. For site s10 there were no observations close to the time of one of soil samples which was taken 29 March 2022.

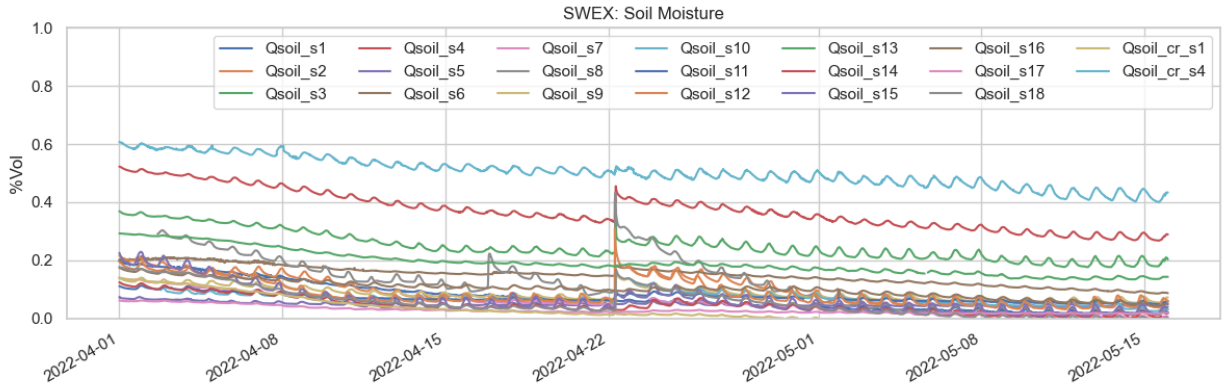

Figure 12. Time series of final Qsoil measurements at each site.

The gravimetric samples also produce values for the bulk density of the soil at each site. These values are shown in **Table 6**.

Table 6. Bulk density, in g/cm^3, of the soil at each site.

Site	Sample 1	Sample 2	Sample 3
s1	1.412	1.273	1.186
s2	1.314	1.653	1.219
s3	1.057	1.358	0.896
s4	1.384	1.332	0.698
s5	0.948	1.040	0.805
s6	0.999	1.365	1.297
s7	1.340	1.224	1.349
s8	1.972	1.854	1.115
s9	1.501	1.380	1.379
s10	1.570	1.538	1.826
s11	1.358	1.456	0.898
s12	0.947	0.887	1.776

s13	0.862	0.855	0.839
s14	1.352	1.481	1.412
s15	0.939	0.632	1.120
s16	0.717	0.583	0.614
s17	1.574	0.459	1.185
s18	1.273	1.544	1.386

Thermal conductivity (Lambda) and Decay time constant (Tau63)

The Hukseflux TP01 measured thermal conductivity and decay time. At site s9 the measurements were bad probably due to improper installation. Data were removed until 5 May 2023 when the sensor was replaced. No other problems noted during operations.

From these measurements, the thermal diffusivity (asoil) and heat capacity of the soil can be calculated. We have included these derived values in the 5-min NetCDF files.

Figure 13. Hukseflux TP01 measurements of soil thermal conductivity (top) and decay time constant (bottom) at each site.

Rain rate, OTT

All sensors performed well. No problems noted during operations. No problems were found during QC processing. No sensors were replaced during operations. Three major rain events have been identified that showed measurable precipitations at more than half the sites (**Table 7)**.

Rainfall event dates and approx. time period
April 11 2100 - April 12 0100 UT
April 16 1800 - 1200 UT
April 22 0300 - 0730 UT

Table 7. Major rainfall events that affected measurements at more than half the sites.

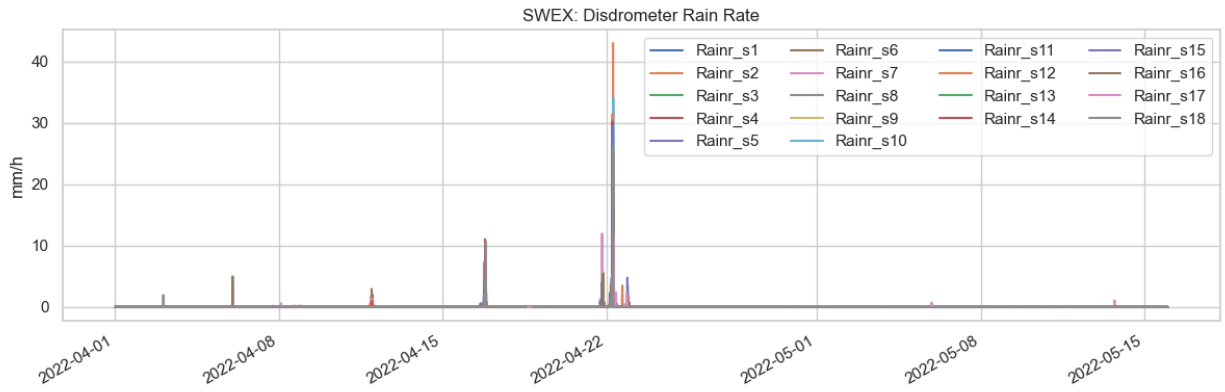

Figure 13. Time series of rain rate at each site.

Intensive Operating Periods (IOP) / Extensive Operating Periods (EOP)

IOP1 - April 4-5 - Eastern Sundowner

IOP2 - April 6-7 - Eastern Sundowner occurring during hot/dry conditions preceding a weak Santa Ana.

IOP3 - April 13-14 - Western Sundowner

EOP1 - April 17 - Western Sundowner

IOP4 - April 18-19 - Western Sundowner

IOP5 - April 23-24 - Eastern Sundowner hybrid with strong winds in the east and west.

EOP2 - April 25-26 - Eastern Sundowner

IOP6 - April 28-29 - Western Sundowner

EOP3 - May 4-5 - Western Sundowner

IOP7 - May 7-8 - Western Sundowner

IOP8 - May 8-9 - Western Sundowner

IOP9 - May 10-11 - Western Sundowner

IOP10 - May 12-13 - Western Sundowner

Appendix A: 2D and 3D Windrose Plot Comparisons

Windrose plots giving an overall comparison between the 10 m 2D and 5m 3D anemometers at each site are provided in the figures below. Overall, despite the height differences, both instruments show comparable direction with the 3D sonics registering higher winds.

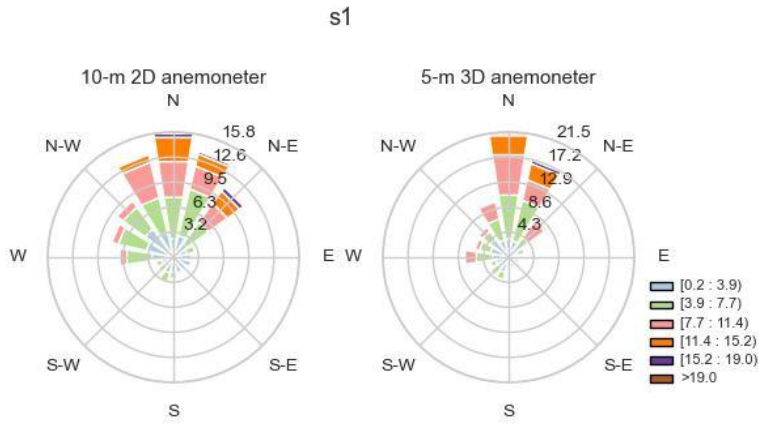

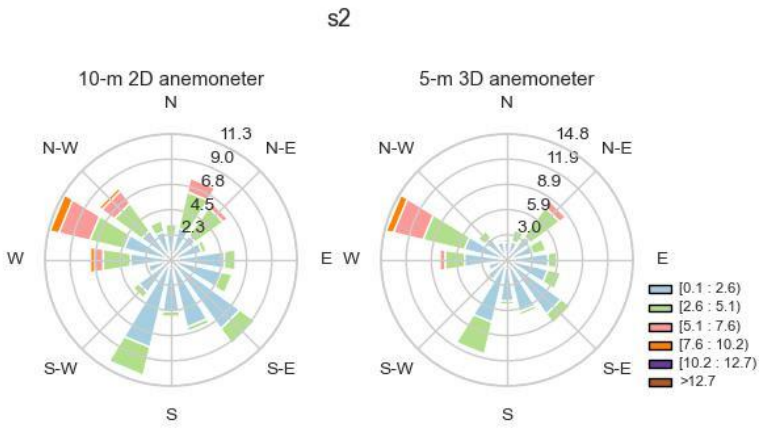

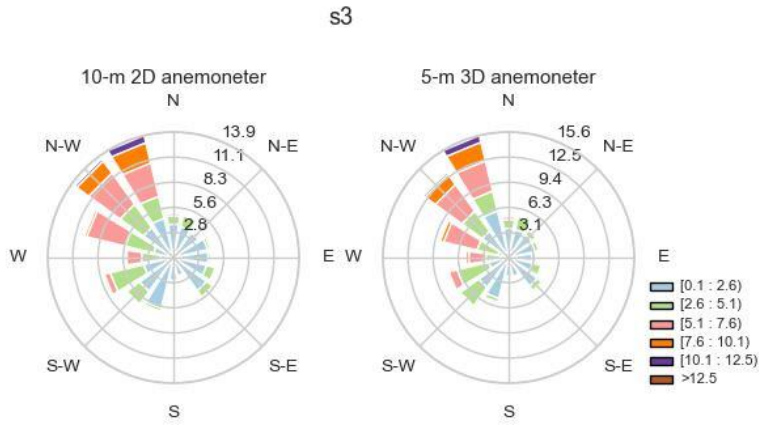

s4

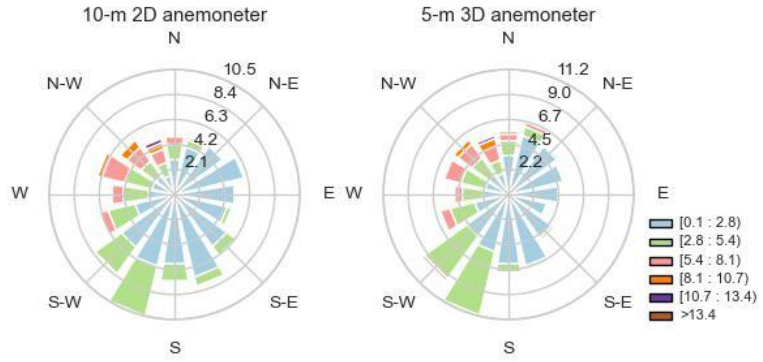
10-m 2D anemometer
N
N-W
N-E
W
E W
E
S-W
S-E
S
10.5
8.4
6.3
4.2
2.1
5-m 3D anemometer
11.2
9.0
6.7
4.5
2.2
[0.1 : 2.8)
[2.8 : 5.4)
[5.4 : 8.1)
[8.1 : 10.7)
[10.7 : 13.4)
>13.4

s5

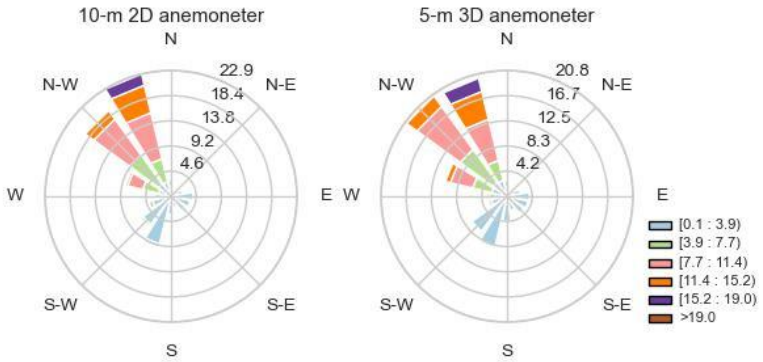
10-m 2D anemometer
N
N-W
N-E
W
E W
E
S-W
S-E
S
22.9
18.4
13.8
9.2
4.6
5-m 3D anemometer
20.8
16.7
12.5
8.3
4.2
[0.1 : 3.9)
[3.9 : 7.7)
[7.7 : 11.4)
[11.4 : 15.2)
[15.2 : 19.0)
>19.0

s6

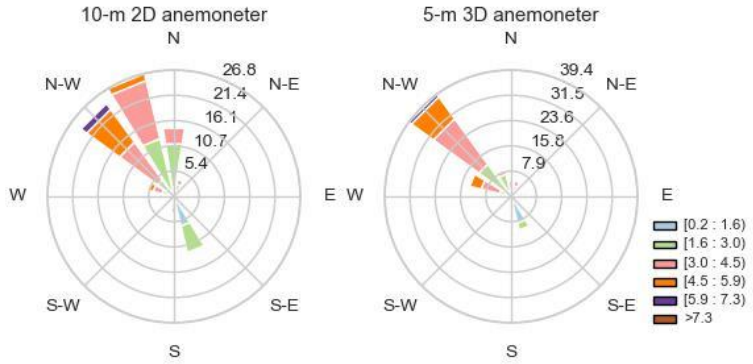
10-m 2D anemometer
N
N-W
N-E
W
E W
E
S-W
S-E
S
26.8
21.4
16.1
10.7
5.4
5-m 3D anemometer
39.4
31.5
23.6
15.8
7.9
[0.2 : 1.6)
[1.6 : 3.0)
[3.0 : 4.5)
[4.5 : 5.9)
[5.9 : 7.3)
>7.3

s7

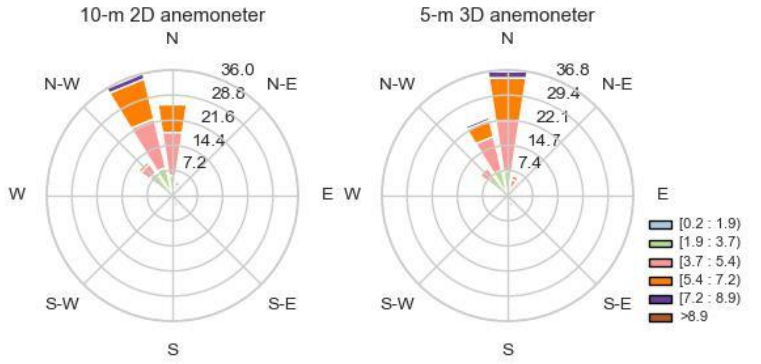
10-m 2D anemometer
N
N-W
N-E
W
E W
S-W
S-E
S
36.0
28.8
21.6
14.4
7.2
5-m 3D anemometer
N
N-W
N-E
E
S-W
S-E
S
36.8
29.4
22.1
14.7
7.4
[0.2 : 1.9)
[1.9 : 3.7)
[3.7 : 5.4)
[5.4 : 7.2)
[7.2 : 8.9)
>8.9

s8

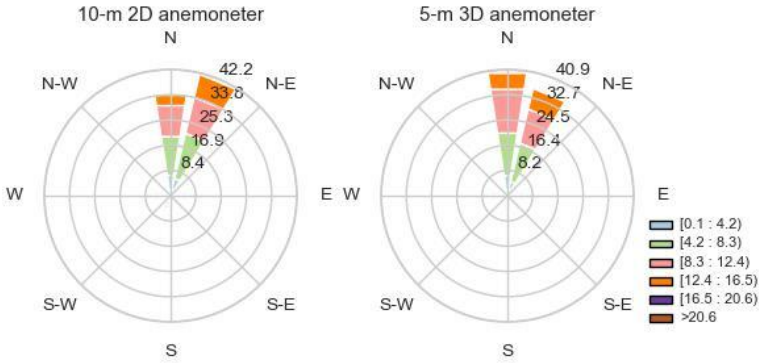
10-m 2D anemometer
N
N-W
N-E
W
E W
S-W
S-E
S
42.2
33.8
25.3
16.9
8.4
5-m 3D anemometer
N
N-W
N-E
E
S-W
S-E
S
40.9
32.7
24.5
16.4
8.2
[0.1 : 4.2)
[4.2 : 8.3)
[8.3 : 12.4)
[12.4 : 16.5)
[16.5 : 20.6)
>20.6

s9

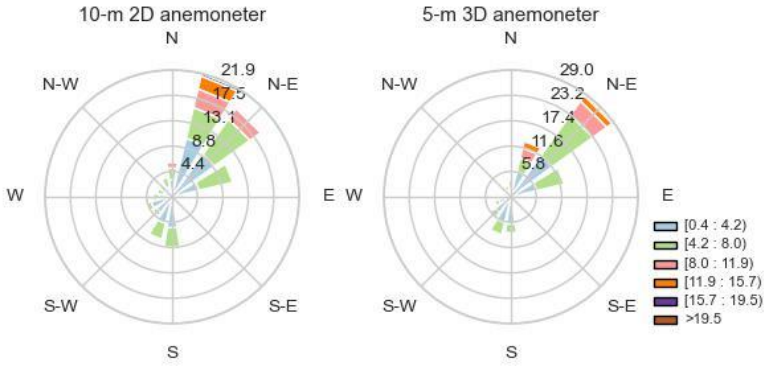
10-m 2D anemometer
N
N-W
N-E
W
E W
S-W
S-E
S
21.9
17.5
13.1
8.8
4.4
5-m 3D anemometer
N
N-W
N-E
E
S-W
S-E
S
29.0
23.2
17.4
11.6
5.8
[0.4 : 4.2)
[4.2 : 8.0)
[8.0 : 11.9)
[11.9 : 15.7)
[15.7 : 19.5)
>19.5

s10

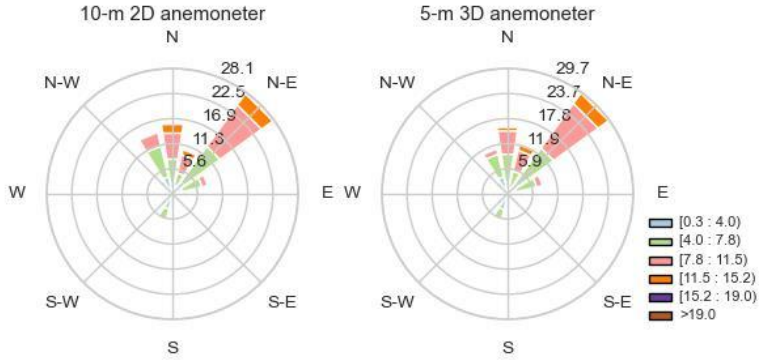
10-m 2D anemometer
5-m 3D anemometer
N
N-E
E
S-E
S
S-W
W
N-W
28.1
22.5
16.9
11.3
5.6
29.7
23.7
17.8
11.9
5.9
[0.3 : 4.0)
[4.0 : 7.8)
[7.8 : 11.5)
[11.5 : 15.2)
[15.2 : 19.0)
>19.0

s11

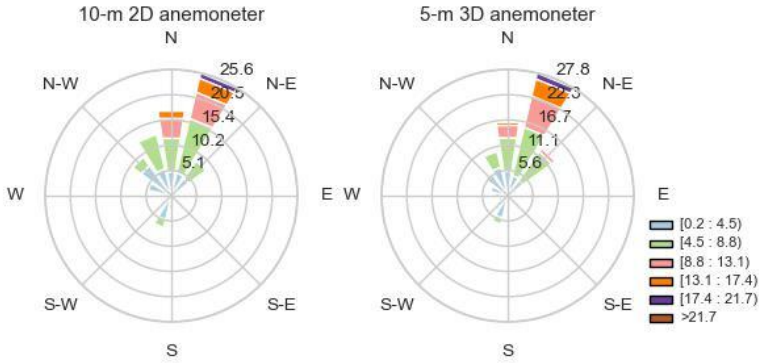
10-m 2D anemometer
5-m 3D anemometer
N
N-E
E
S-E
S
S-W
W
N-W
25.6
20.5
15.4
10.2
5.1
27.8
22.3
16.7
11.1
5.6
[0.2 : 4.5)
[4.5 : 8.8)
[8.8 : 13.1)
[13.1 : 17.4)
[17.4 : 21.7)
>21.7

s12

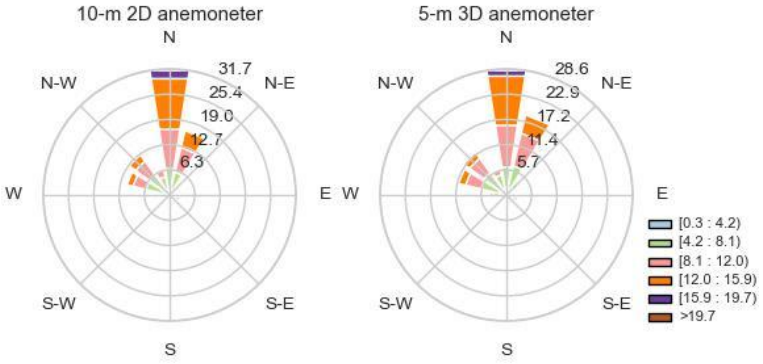
10-m 2D anemometer
5-m 3D anemometer
N
N-E
E
S-E
S
S-W
W
N-W
31.7
25.4
19.0
12.7
6.3
28.6
22.9
17.2
11.4
5.7
[0.3 : 4.2)
[4.2 : 8.1)
[8.1 : 12.0)
[12.0 : 15.9)
[15.9 : 19.7)
>19.7

s13

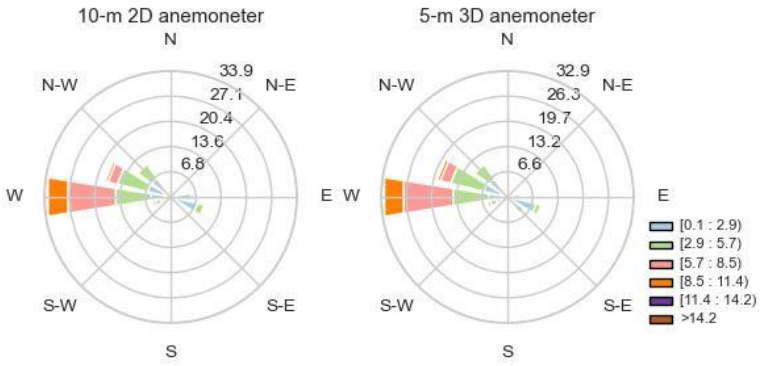
10-m 2D anemometer
N
N-E
E
S-E
S
S-W
W
N-W
33.9
27.1
20.4
13.6
6.8
5-m 3D anemometer
32.9
26.3
19.7
13.2
6.6
[0.1 : 2.9)
[2.9 : 5.7)
[5.7 : 8.5)
[8.5 : 11.4)
[11.4 : 14.2)
>14.2

s14

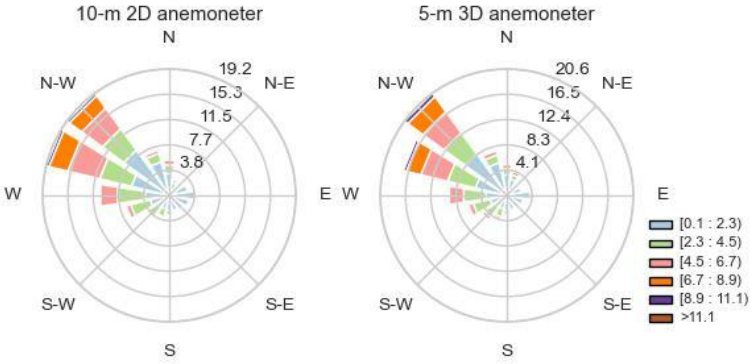
10-m 2D anemometer
N
N-E
E
S-E
S
S-W
W
N-W
19.2
15.3
11.5
7.7
3.8
5-m 3D anemometer
20.6
16.5
12.4
8.3
4.1
[0.1 : 2.3)
[2.3 : 4.5)
[4.5 : 6.7)
[6.7 : 8.9)
[8.9 : 11.1)
>11.1

s15

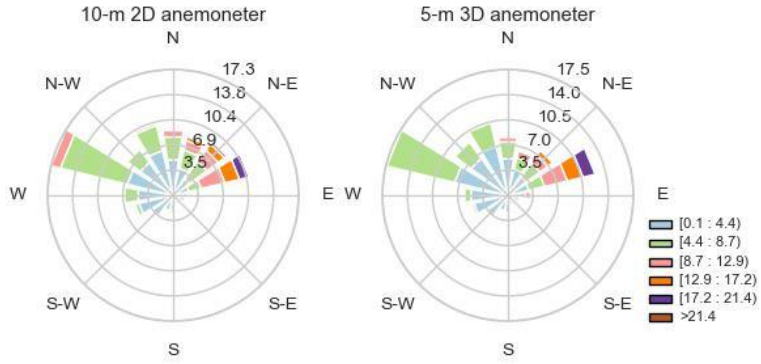
10-m 2D anemometer
N
N-E
E
S-E
S
S-W
W
N-W
17.3
13.8
10.4
6.9
3.5
5-m 3D anemometer
17.5
14.0
10.5
7.0
3.5
[0.1 : 4.4)
[4.4 : 8.7)
[8.7 : 12.9)
[12.9 : 17.2)
[17.2 : 21.4)
>21.4

s16

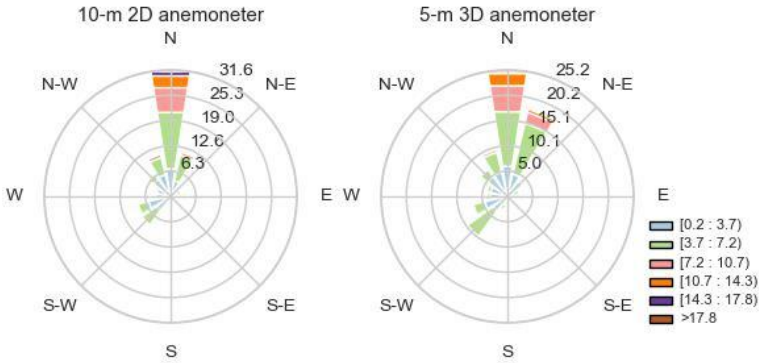
10-m 2D anemometer
N
N-W
N-E
W
E W
S-W
S-E
S
31.6
25.3
19.0
12.6
6.3
5-m 3D anemometer
25.2
20.2
15.1
10.1
5.0
E
[0.2 : 3.7)
[3.7 : 7.2)
[7.2 : 10.7)
[10.7 : 14.3)
[14.3 : 17.8)
>17.8

s17

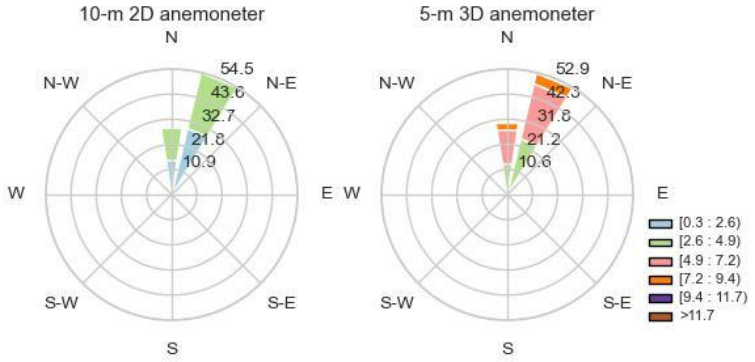
10-m 2D anemometer
N
N-W
N-E
W
E W
S-W
S-E
S
54.5
43.6
32.7
21.8
10.9
5-m 3D anemometer
52.9
42.3
31.8
21.2
10.6
E
[0.3 : 2.6)
[2.6 : 4.9)
[4.9 : 7.2)
[7.2 : 9.4)
[9.4 : 11.7)
>11.7

s18

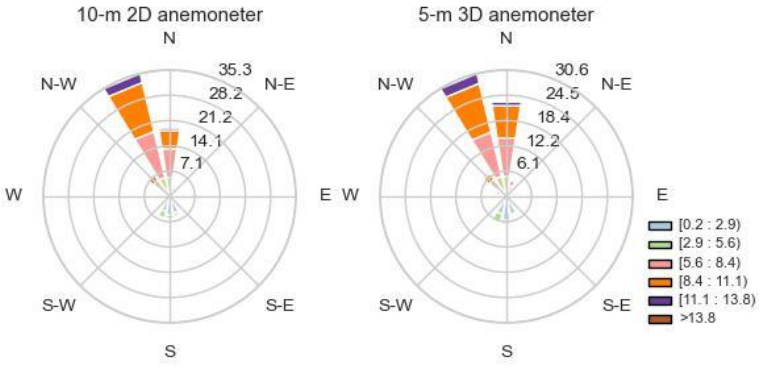
10-m 2D anemometer
N
N-W
N-E
W
E W
S-W
S-E
S
35.3
28.2
21.2
14.1
7.1
5-m 3D anemometer
30.6
24.5
18.4
12.2
6.1
E
[0.2 : 2.9)
[2.9 : 5.6)
[5.6 : 8.4)
[8.4 : 11.1)
[11.1 : 13.8)
>13.8